CONF-901071--3

DISCLAIMER

Ion-Beam-Assisted Deposition of Silver Films on Zirconia Ceramics for Improved Tribological Behavior

A. Erdemir, D.E. Busch, R.A. Erck, G.R. Fenske and R. Lee
Tribology Section
Materials and Components Technology Division
Argonne National Laboratory
Argonne IL 60439

CONF-901071--3

DE90 009706

To be presented at the Joint STLE-ASME Tribology Conference
Toronto, Canada
7-10 October 1990

ION-BEAM-ASSISTED DEPOSITION OF SILVER FILMS ON ZIRCONIA CERAMICS FOR IMPROVED TRIBOLOGICAL BEHAVIOR*

A. Erdemir (STLE), D. E. Busch, R. A. Erck (STLE),
G. R. Fenske (STLE), and R. Lee
Tribology Section
Materials and Components Technology Division
Argonne National Laboratory
Argonne, IL 60439

ABSTRACT

Silver coatings of 2 μm nominal thickness were deposited on toughened zirconia ceramics by ion-beam-assisted deposition (IBAD). Tribotests were performed with ball-on-disk machines under a load of 5 N, at velocities of 0.1 to 2 $m.s^{-1}$, and in dry and normal air. The sliding friction coefficients of zirconia on itself ranged from 0.3 to 1.2, and the wear rates spanned more than three orders of magnitude, depending on the sliding velocity. In contrast, the wear of IBAD-silver-coated disks was practically unmeasurable, and the wear of zirconia balls was reduced by factors of 5 to 1200 below that of balls slid against uncoated zirconia disks. Large reductions in friction coefficients were also observed for the pairs that included an IBAD-silver film. Scanning-electron microscopy and laser-Raman spectroscopy were used to elucidate the mechanisms of wear of coated and uncoated ceramics.

* Work supported by the Tribology Program, U.S. Department of Energy, Energy Conversion and Utilization Technologies Division, under Contract W-31-109-Eng-38.

INTRODUCTION

Transformation-toughened zirconia ceramics, mainly because of their excellent strengths, high fracture toughness, and good insulating nature, are being considered for use in fuel-efficient energy conversion and utilization devices, most notably the low-heat-rejection-engines (LHRE) (1-6). It is believed that with the use of these ceramics, uncooled engine systems will become feasible and their adiabatic efficiency will increase substantially (4-6). Despite the attractive properties offered by zirconia ceramics, their immediate use in engine applications appears very unlikely, mainly because of their poor wear performance and high friction coefficients even under oil-lubricated sliding conditions (4,5).

The current state of the art in the tribology of zirconia-based ceramics suggests that the poor wear performance of these materials is often associated with their inability to conduct heat rapidly and to resist thermal shock adequately (3-5, 7,8). It is known that essentially all the mechanical work done to overcome friction is converted into heat that is confined primarily to the areas of real contact. Because of the very low thermal conductivity of zirconia ceramics, large temperature gradients are generated between local areas and surrounding regions; these in turn create high thermal stresses. Due to the inherently low thermal shock resistance of zirconia, microcracks may eventually develop at the rubbing interfaces and increase wear. Woydt and Habig showed that the total

volumetric wear coefficient of self-mated MgO-partially stabilized zirconia (MgO-PSZ) couples increased more than three orders of magnitude when sliding velocity was raised from 0.03 to 1 $m.s^{-1}$ (7,8). Wear studies by Aronov (9) and Aronov and Benetatos (10) presented further evidence that increasing temperatures and sliding velocities were very influential on the wear performance of transformation-toughened zirconia ceramics (9,10).

In recent years, a few attempts have been made to improve the generally poor wear performance of zirconia ceramics. Lankford et al. (1) and Wei et al. (2,11) used ion-beam mixing to change the near-surface chemistry of PSZ ceramics. After mixing Ti, Ni, and/or Co layers with PSZ surfaces, they achieved friction coefficients of 0.06 to 0.09 at 800°C, but the wear rates they measured were quite high. Aronov and Benetatos employed laser-beam treatment to increase the wear resistance of MgO-PSZ ceramics (10). They found that under optimized laser-beam conditions, significant improvements in both the hardness and wear of these ceramics were feasible. Recently, Erdemir et al. have undertaken a different approach for achieving low wear in ceramics, particularly in those with poor thermal conductivity (12). They proposed that thin metallic films combining high thermal conductivity with low shear strength can improve the wear performance of ceramics, because, as was evident from the previous studies, the poor wear performance of these materials was largely dominated by their inability to dissipate frictional heat from the rubbing surfaces. Thin films of

silver and gold appear very promising, because their thermal conductivities (k) are very high (e.g., at 298 K, k_{silver} = 4.29 $W.cm^{-1}.K^{-1}$, k_{gold} = 3.17 $W.cm^{-1}.K^{-1}$) and their shear strengths are low. Copper, because of its high thermal conductivity (e.g., k_{copper} = 4.01 $W.cm^{-1}.K^{-1}$), may also be considered; compared to gold and silver, however, it lacks the high chemical inertness that is essential for long-term service. The low shear strength of silver and gold can reduce friction, which in turn reduces the probability of microcrack initiation in these inherently brittle solids, as demonstrated in ref. (13).

Recent tribological studies by Erdemir et al. have indicated that through the use of silver films, wear of alumina disks could virtually be eliminated; balls sliding against these disks experienced more than two orders of magnitude lower wear than those slid against the uncoated disks, depending on ambient temperature and sliding velocity (13,14). The rubbing surfaces of pairs without the silver films appeared to have undergone severe microfracture, plastic flow, and even local melting, depending on test conditions. No such characteristics were seen on the sliding surfaces of pairs that incorporated a silver film. In this study, an attempt was made to further explore the effectiveness of thin silver films in controlling the wear of transformation-toughened zirconia ceramics. Combining high thermal conductivity with low shear strength, silver is expected to have a more beneficial effect on the wear of zirconia ceramics than it had on that of alumina because, compared

to that of alumina, the thermal conductivity of most toughened zirconia ceramics is much lower (e.g., $k_{alumina}$ = 0.25 $W.cm^{-1}.K^{-1}$, $k_{zirconia}$ = 0.02 $W.cm^{-1}.K^{-1}$).

EXPERIMENTAL DETAILS

Test Materials

The disk specimens used in this study were fabricated from calcia-stabilized tetragonal zirconia by sintering at 1800°C. According to the technical data provided by the manufacturer (15), the principal constituent, ZrO_2 (99 wt.%) was doped with CaO (5 wt.%). Volume porosity of the end products was less than 1%. The Knoop hardness of the zirconia disks was approximately 15 GPa. The disk specimens, 50 mm in diameter by 6 mm thick, were surface-finished by diamond-wheel grinding to an average roughness value of 0.2 ± 0.02 µm center-line average (CLA).

The counterface pins were made of 9.5-mm diameter CaO-stabilized zirconia balls with a surface finish of about 0.03 µm CLA. They were firmly secured on a holder to assume the stationary ball configuration of the ball-on-disk machine used in this study. All specimens were ultrasonically cleaned sequentially in hexane + 10 vol.% toluene, acetone, deionized water containing 2 wt.% laboratory detergent, and deionized water for about 1 min each,

then dried in an oven at 110°C for 20 min. This cleaning sequence was shown in Ref. 16 to remove much of the organic contamination from the exposed surfaces of oxide ceramics.

Ion-Beam-Assisted Deposition (IBAD) of Silver

The IBAD of thin silver films (e.g., approximately 2 μm thick) was performed at room temperature in a vacuum chamber equipped with an electron-beam-heated evaporation source. A mixture of argon and oxygen gas was fed through the ion source to create an ion flux composed of the ions of these gases. To remove the adsorbed contaminants from the surface, the substrates were subjected to Ar + O ion bombardment at an acceleration voltage of 1 keV before evaporation of the silver. The thickness of the growing film was controlled with the aid of a quartz-crystal rate monitor. Ion bombardment of the growing films was achieved with a hot-cathode Kaufman-type ion gun. Acceleration voltage and ion current density were 25 $\mu A.cm^{-2}$ and 1 keV, respectively, during silver deposition. The ions were neutralized by a hot-wire filament, thereby reducing the charging of insulating ceramic substrates. After a 1000-Å-thick film was produced under ion bombardment, the ion beam was turned off and the gas flow through the ion source was stopped. The balance of the film thickness was obtained by vacuum evaporation. Further details of this system, together with the structural characteristics of resultant films, were elaborated in previous publications (12,13,17).

Friction and Wear Tests

Friction and wear were tested with the pairs of zirconia balls and disks and zirconia balls and IBAD-silver coated zirconia disks in two ball-on-disk tribometers. The specific test conditions for each experiment are summarized in Table 1. Most tests were run in dry air of less than 1% relative humidity. A few pairs with and without silver films were wear-tested in normal air of 18 ± 2% relative humidity, primarily to assess and compare the long-term tribological performance of IBAD-silver films to that of pairs without a silver film. The dead weight applied on top of the ball specimens was 5 N which created an initial mean Hertzian contact pressure of approximately 0.46 GPa and an elastic contact radius of about 58 μm between the ball and disk specimens. Frictional force was monitored with the aid of linear variable-displacement-transducers and recorded on chart papers throughout the tests.

Wear-volume measurements on the balls used a mathematical expression suggested by Fischer and Tomizawa (18). The wear of disk specimens was assessed from the traces of surface profiles across the wear tracks. For better accuracy and reproducibility, two to three duplicate tests were run, and the average values with the spread are reported. Wear scars and tracks, as well as wear-debris particles, were examined with scanning electron microscopy and laser-Raman spectroscopy. To reduce charging during electron-

microscopy inspection, a thin carbon film (about 10 nm thick) was vapor-deposited on the surfaces of ceramic pieces.

RESULTS

Friction

Table 2 presents the friction coefficients of all pairs measured at different sliding velocities. In general, both the initial and steady-state friction coefficients of pairs without the silver films increased with increasing velocity. The pairs tested at 0.1 $m.s^{-1}$ exhibited high friction coefficients initially (e.g., about 0.6), but distinctly low friction coefficients at steady states (e.g., 0.3). In contrast, the pairs tested at 0.3, 0.5, 1, and 2 m/s displayed average friction coefficients of 0.55 to 1.1 initially and 0.75 to 1.2 at steady state. In general, the friction coefficient tended to increase with increasing velocity. During sliding at 2 $m.s^{-1}$, a continuous streak of light was seen at the sliding interface and discontinuous flashes were visible to the unaided eye even with the room light on.

As shown in Table 2, the friction coefficients of pairs with an IBAD-silver film ranged from 0.40 to about 0.45 at steady state. Increasing the velocity and sliding distance did not alter these values significantly. Initially, the friction coefficients of pairs involving a silver film were 0.2 to 0.35.

Figure 1 shows the range of the friction coefficients of pairs with and without the silver films during sliding in long-term tests. At steady state, the friction coefficient of pairs without the silver films is approximately 0.8. In contrast, the friction coefficient of pairs with the silver films was about 0.43 and remained steady up to a sliding distance of about 78 km (e.g., 600,000 revolutions). With further sliding, the friction coefficient tended to increase before stabilizing at about 0.58 beyond a sliding distance of 90 km.

Wear

The wear rates of various test pairs, measured as a function of sliding velocity, are shown in Figure 2. As is evident, the wear of balls and disks increased dramatically with increasing velocity. For instance, an increase in sliding velocity from 0.1 to 2 $m.s^{-1}$ gave rise to a wear rate increase in balls on the order of 3500 times. Disk wear also increased substantially when the velocity was increased from 0.1 to 1 $m.s^{-1}$. However, a slight decrease was seen in disk wear rate when the velocity was further increased to 2 $m.s^{-1}$.

For pairs with an IBAD-silver film, the wear rates of balls were reduced by factors ranging from 5 at 0.1 $m.s^{-1}$ to more than 1000 at 1 and 2 $m.s^{-1}$. Wear of disks coated with IBAD-silver was essentially unmeasurable. Attempts were made to assess the extent of wear on

these disks by a surface profilometer, but failed to yield any reliable wear data. As will be shown later, wear appeared to have been confined to the asperity tips of underlying substrates.

The balls slid against the uncoated disks during wear-life tests displayed wear rates of approximately 6.1×10^{-5} $mm^3.N^{-1}.m^{-1}$, whereas the wear rate of balls sliding against the silver-coated disks was about 3.8×10^{-7} $mm^3.N^{-1}.m^{-1}$. The extent of wear on the disk having slid 78 km is illustrated in Figs. 3a and 3b. These 3-D surface maps were generated by the profilometer by repeatedly scanning the diamond stylus across the wear tracks. Loss of material from the wear track of the uncoated surface appears quite high. However, the surface map for the silver-coated disk suggests very little material loss from this track. A back-scattered electron micrograph of this track and the corresponding silver X-ray map are shown in Figs. 4a and 4b, respectively. These photographs indicate that silver had been removed from the center part of the wear track but was still present on the sides.

Wear-Surface Analyses

The electron micrographs in Fig. 5 show the general conditions of the wear scars formed on the balls during sliding against the uncoated disks at different velocities. It is clear that the wear-scar diameter increases markedly with increasing velocity. At higher magnifications, the wear scar of balls tested at 0.1 $m.s^{-1}$ appears quite smooth, as shown in Fig. 6a. The scars formed at higher sliding velocities (e.g., 0.5, 1, and 2 $m.s^{-1}$) exhibited microfeatures indicative of plastic flow (denoted with an arrow in Fig. 6b), microcracks (see Fig. 6c), and certain features that suggest localized melting (denoted with an arrow in Fig. 6d). Colonies of flake-like wear fragments were present on the worn surfaces (Fig. 7a) and around the trailing edges of balls tested at 2 $m.s^{-1}$ (Fig. 7b)

The wear tracks formed on the disk sides exhibited microfeatures similar to those exhibited by their respective ball counterparts. Typically, plastic flow was evident on all surfaces, but extensive microcracks were seen primarily on surfaces tested at higher velocities. Fig. 8a shows the surface condition of a track formed at 0.1 $m.s^{-1}$. Like the ball side (see Fig. 6a) It appeared smooth and consisted of some features suggesting plastic flow. Fig. 8b presents the wear-surface morphology of a track formed at 1 $m.s^{-1}$. Microcracks and plastic flow appear to be the dominant features of the wear scars formed at 1 $m.s^{-1}$. At 2 $m.s^{-1}$, the worn surfaces

contained microfeatures suggesting plastic flow, microcracks, and even some melting, as denoted in Fig. 8c. Wear-debris particles collected from the worn surfaces were a combination of flake-like fragments (Figs. 7a and 8b) and sub-micrometer-size, powder-like particles (Fig. 9).

For the pairs including silver films, electron-microscopy inspection revealed that silver films remained intact on the wear tracks. As shown in Fig. 10a, only the tips of underlying asperities were exposed. Figure 10b suggests that wear was largely confined to the exposed tips of surface asperities. As discussed earlier, a quantitative assessment of wear in these silver-coated disks was essentially impractical with the use of a surface profilometer. The balls slid against these disks had much smaller wear scars than those slid against the uncoated disks, as can be seen in Fig. 11. At high magnifications, all of the wear scars appeared very smooth, free from any clear indications of the plastic flow, microcracking, or melting, typically seen on the scars of balls slid against the uncoated disks.

DISCUSSION

The results presented above demonstrate that the wear of CaO-stabilized tetragonal zirconia ceramics increases dramatically with increasing sliding velocity. This observation is consistent with those of Woydt and Habig (7) and Ishigaki et al. (19). Furthermore, thin silver films produced in this study can markedly reduce both the wear and friction coefficients of zirconia ceramics subjected to short- (see Fig. 2 and Table 2) and long-distance sliding tests (see Figs. 1 and 3). The latter finding supports the hypothesis that thin films with high thermal conductivity can indeed reduce the wear of insulating ceramics (12).

Friction and Wear of Uncoated Surfaces

Steady state friction coefficients measured at 0.1 $m.s^{-1}$ were rather low, e.g., 0.32, and rubbing surfaces appeared very smooth, as evident from Figs. 5a, 6a, and 7a. We believe that these two observations were interrelated. The friction coefficient was low, largely because the ploughing component of friction was insignificant on these smoother surfaces. Low friction at lower velocities was also measured by Hannink et al. (20) and Yust and Carignan (21) between sliding surfaces of toughened-zirconia ceramics. Relatively high friction coefficients (e.g., 0.6) measured on pairs at the start of tests can be attributed to an initially rough surface (e.g., 0.2 µm CLA for disks). We believe

that the ploughing component of friction was high on these initially rough surfaces. As the surface became increasingly smooth during successive sliding passes (known as running-in process), the ploughing component decreased, thereby reducing friction.

As for the low wear of balls and disks tested at 0.1 $m.s^{-1}$ (Fig. 2), we believe that low friction and velocity, together with the ability of these ceramics to undergo some plastic deformation, were the dominant factors. As reported by Hamilton and Goodman (22), the location and orientation of subsurface stress fields are altered by friction between sliding bodies. At lower friction coefficients, the surface tensile stresses that generate behind the moving asperities are relatively small. Therefore, low steady-state friction at 0.1 $m.s^{-1}$ was insufficient to create adequate surface tensile stresses that could initiate microfracture. Instead, frictional force was accommodated by some plastic deformation exhibited by tough zirconia test pairs (see Fig. 8a). There was no indication of tensile-crack formation on these surfaces. As for the frictional heating of sliding interfaces causing thermal cracking, we believe that because of low friction and velocity, the amount of frictional heat flux that was generated at these sliding interfaces was low. The reason is that the amount of frictional heat flux, q, is proportional to the friction coefficient, μ, the normal force, F, and sliding velocity, v, but inversely proportional to the nominal contact area, A_n, as given by $q = (\mu.F.v)/A_n$ (23). Therefore, the generation of thermal and/or thermomechanical cracks

was also unlikely at this low velocity. We believe that wear was controlled largely by a deformation mechanism, as suggested by the electron microscopy of the surfaces rubbed at 0.1 $m.s^{-1}$ (see Figs. 6a and 8a).

At higher velocities, our results indicate that friction and wear of zirconia test pairs increase dramatically. For high friction coefficients, we propose the following interpretation. Because of the higher velocities, the amount of frictional heat flux generated at the sliding interfaces was much higher than that generated at 0.1 $m.s^{-1}$. As a result, local softening and even microwelding may have occurred between asperities of the opposing surfaces. This is known to increase the adhesive component of frictional force. In Table 2, it was shown that the friction coefficient increased substantially with velocity. This observation further supports the above interpretation by suggesting that perhaps both the number and area of microwelding causing adhesion between opposing asperities had increased. Observation of microfeatures suggesting plastic flow and some limited melting on sliding surfaces (see Figs, 6b, 6d, 8b, and 8d) is consistent with the explanation provided above. Viewing the micrographs taken from these sliding surfaces, one also notices that these surfaces were rougher than those tested at 0.1 $m.s^{-1}$ (Figs. 6 and 8). Therefore, it is reasonable to believe that in these test pairs, the ploughing component of frictional force was also high.

Higher wear rates observed at 0.5, 1, and 2 m/s sliding velocities are attributable to increasing frictional heating at the sliding interfaces of these test pairs. Because of the very low thermal conductivity of base material, frictional heat cannot be dissipated rapidly. This may cause these areas to reach very high temperatures, (known as flash temperatures). Because of a steep temperature gradient between these and surrounding areas, high thermal stresses are generated. Inherently low thermal-shock resistance may cause microcracks to develop eventually and with the aid of surface contact stresses, wear occurs. This interpretation is consistent with the thermomechanical wear theory of ceramics proposed by Winer and Ting (24) and with the interpretation of Dufrane and Glaeser (3,4), who examined wear behavior of zirconia ceramics in environments similar to those of actual heat engines. We also believe that surface tensile stresses generated behind the moving asperities were relatively high at these high velocities. As argued earlier, this situation gives rise to the formation of tensile cracks on sliding surfaces, and the electron micrographs in Figs. 6b, 6c, 8b, and 8c support this interpretation by revealing microcracks oriented perpendicularly to the sliding direction.

Although their role in the wear of zirconia ceramics tested in our study has not yet been clearly understood, microfeatures typical of local melting (see Figs. 6d and 8c) were seen on the surfaces rubbed at 2 $m.s^{-1}$. Higher wear rates measured at this velocity can be attributed in part to this local melting because microscopic

inspection of surfaces rubbed at 2 $m.s^{-1}$ revealed flat wear fragments on and around the wear scars (Figs. 7a and 7b), as well as among the wear-debris particles (Fig. 9) collected from these surfaces. The large fragments in Fig. 7b appear to have been forced out of the sliding interface in the molten state, after which they solidified and accumulated around the trailing edge of the rubbing ball. Thermal calculations are underway to substantiate these tentative conclusions on the effect of sliding velocity.

Regarding the possibility of a thermal and/or stress-induced phase transformation leading to microcrack formation, and hence wear, we analyzed the rubbing surfaces by micro-laser-Raman spectroscopy. The data gathered so far indicated that the tetragonal crystalline phase of the as-received ceramic was not altered by the stresses and/or frictional heat generated under the test conditions in this study. Therefore, a mechanism leaning toward the phase-transformation-induced-wear was not well-founded in our study. It is possible that the tetragonal phase may have transformed into monoclinic phase but may have been removed from the surface by dynamic rubbing and/or transformed back to the tetragonal phase. Based on laser-Raman spectroscopy observations, Ishigaki et al. (19) could not also find any trace of monoclinic phase on yttria-PSZ ceramics with predominantly tetragonal phase. Stress- and temperature- induced phase transformations (e.g., tetragonal to monoclinic, tetragonal to cubic, and back to tetragonal etc.) have been observed on various partially stabilized zirconia (PSZ)

ceramics subjected to wear testing (7,9,10,25) and grinding (26). Aronov (9), Woyd and Habig (7), and Birkby et al. arguded that since such transformations involve volume shrinkage and/or dilation on rubbing surfaces, high tensile and/or compressive stresses can generate. Cyclic occurrence of these events may initiate cracks, thus promoting wear in these ceramics.

Friction and Wear of Pairs, Including IBAD-Silver Films

As shown in Table 2, IBAD-silver films substantially reduced the friction coefficients of zirconia test pairs tested at 0.5, 1, and 2 $m.s^{-1}$. We believe that the low shear strength of silver was primarily responsible for the low friction. Under tangential loading, which is analogous to low friction, this film shears easily. However, strong film-to-substrate adhesion imparted by IBAD was of critical importance in achieving not only longer wear lives but also for maintaining the low friction coefficients for sliding distances as long as 78 km (see Fig. 1). Using a pull-type adhesion tester, we were unable to separate the IBAD-silver films from their substrates. The bonding agent between the pull stub and the IBAD silver film failed before the film was removed. The bonding agent had a tensile strength of about 70 MPa; this means that the silver films developed on zirconia ceramics had adhesion strengths higher than 70 MPa. Furthermore, the wear test itself can be considered as a type of adhesion test, as was demonstrated in Ref. 12. (For further insight into the mechanisms of strong film adhesion

afforded by the IBAD process, readers should refer to a handbook edited by Cuomo et al. [27]). In short, these IBAD-silver films have proven themselves adherent enough to endure both the normal and tangential components of the surface contact stresses generated during the sliding contacts in the tests performed here.

The low wear rates of balls sliding against the silver-coated disks (see Fig. 2) can be attributed to increased lateral thermal conductivity imparted to the rubbing surfaces by the silver films. Note that the thermal conductivity of silver is 214 times higher than that of zirconia tested in this study. Using an infrared camera, Griffioen et al. recently measured flash temperatures above 2000°C on the rubbing interface of a sapphire disk and a silicon nitride ball (tip radius = 3.18 mm) (28). The sliding velocity and the normal force used in their experiment were 1.5 $m.s^{-1}$ and 4.45 N, respectively. Although the range of flash temperatures generated during our wear tests is not yet known, our electron-microscopy observations lead us to believe that at sliding velocities of 0.5, 1, and 2 $m.s^{-1}$, at least the flash temperatures were high, because some evidence of local melting was seen on rubbing surfaces (see Fig. 6d). It should be noted that the thermal conductivity of zirconia is markedly lower than that of silicon nitride and sapphire. Therefore, we believe that much lower wear rates of balls (e.g., more than three orders of magnitude at 1 and 2 $m.s^{-1}$) were due largely to the rapid dissipation of frictional heat from the asperity contacts of these sliding interfaces. In addition, since

silver shears easily, the tensile forces giving rise to surface cracks on rubbing surfaces were also reduced.

The unmeasurable wear losses on the silver-coated disks are believed to be due largely to the excellent adhesion of IBAD-silver films. In Fig. 10b, the silver film appeared intact on the wear track, but shear deformation had taken place to accommodate the normal and tangential forces generated during sliding contact. Note that only the summits of the substrate asperities (appearing as dark areas in the micrograph) are visible. As mentioned earlier, a quantification of the material loss on these silver-coated disks was virtually impossible with a surface profilometer.

CONCLUSIONS

1. Under the test conditions explored in this study, dry sliding of CaO-stabilized tetragonal zirconia ceramics on themselves causes high friction and wear losses. Increased sliding velocities are particularly detrimental to the wear behavior of these ceramics.

2. Based on electron-microscopy observations, thermal and/or thermomechanical instabilities are the major sources of wear in zirconia ceramics used in this study. Thermal cracks, plastic flow, and local melting were typical characteristics of the rubbing surfaces.

3. Because of their low shear strength and high thermal conductivity, silver films virtually eliminated the wear of flats and reduced the wear of counterface balls by factors of 5 to more than 1200. Furthermore, thin silver films significantly reduced the friction coefficients of zirconia ceramics. The friction- and wear-reducing capability of silver films becomes even more pronounced at higher sliding velocities.

4. When these and other insulating ceramics are considered for heat-engine and other tribo-applications, it is important that the thermal and/or thermomechanical instabilities of these ceramics be recognized as serious. As demonstrated in this study, the use of an adherent metal film combining a high thermal conductivity with a low shear strength and good chemical inertness appears promising for advanced tribological applications using ceramics.

ACKNOWLEDGEMENT

The authors thank Dr. J. C. Parker of the Materials Science Division at Argonne National Laboratory for providing the laser-Raman-spectroscopy data.

Table 1. Friction and wear test conditions for test pairs.

Parameters	Wear Tests	
	Dry Air	Normal Air
Load (N)	5.0	5.0
Sliding velocity ($m.s^{-1}$)	0.1 to 2.0	1.0
Relative humidity (%)	0	18 ± 2
Sliding distance (km)	2	78 to 100
Wear-track diameter (mm)	35 to 41	40 ± 2
Ambient temperature (°C)	23 ± 1	23 ± 1
Number of tests	3	2
Tip radius of balls (mm)	4.8	4.8
Diameter of disks (mm)	50	50

Table 2. Friction coefficients of pairs with and without an IBAD-silver film at various sliding velocities.

Sliding Velocity ($m.s^{-1}$)	Zirconia/Zirconia		Zirconia/Ag-Coated-Zirconia	
	Initial	Steady-state	Initial	Steady-State
0.1	0.6 ± 0.05	0.32 ± 0.1	0.35 ± 0.05	0.40 ± 0.05
0.3	0.5 ± 0.05	0.75 ± 0.06	-	-
0.5	0.7 ± 0.1	0.8 ± 0.05	0.3 ± 0.05	0.41 ± 0.05
1.0	0.7 ± 0.05	0.81 ± 0.05	0.2 ± 0.1	0.42 ± 0.05
2.0	1.1 ± 0.1	1.20 ± 0.1	0.2 ± 0.7	0.45 ± 0.05

REFERENCES

(1) Lankford, J., Wei, W., and Kossowsky, R., "Friction and Wear Behavior of Ion-beam-modified Ceramics," J. Mater. Sci., 22, pp 2069-2078 (1987).

(2) Wei, W., Lankford J., and Kossowsky, R., "Friction and Wear of Ion-beam-modified Ceramics for Use in High Temperature Adiabatic Engines," Mat. Sci. Eng., 90, pp 307-315 (1987).

(3) Dufrane, K. F., and Glaeser, W. A., "Performance of Ceramics in Ring-Cylinder Applications," Int. Congr. and Exposition, Detroit, SAE preprint 870416 (February 23, 1987).

(4) Dufrane, K. F., and Glaeser, W. A., "Wear of Ceramics in Advanced Heat Engine Applications," Int. Conf. on Wear of Materials, ASME, New York (1987) Ed. Ludema, K.C., pp 285-291.

(5) Dufrane, K. F., "Wear Performance of Ceramics in Ring/Cylinder Applications," Ceram. Eng. Sci. Proc., 9, pp 1409-1418 (1988).

(6) Kamo, R., Woods, M., and Sutor, P., "Development of Tribological System and Advanced High-Temperature Diesel Engines," Proc. of the Coatings for Advanced Heat Engine Workshop, pp 73-92 (1987).

(7) Woydt, M., and Habig, K.-H., "High Temperature Tribology of Ceramics," Tribol. Int., 22, pp 75-88 (1989).

(8) Woydt, M., and Habig, K.-H., "Influence of Temperature and Sliding Speed on Friction and Wear of SiSic and MgO-ZrO_2," Ceram. Eng. Sci. Proc., 9, pp 1419-1430 (1988).

(9) Aronov, V., "Friction Induced Strengthening Mechanisms of Magnesia Partially Stabilized Zirconia," J. Tribol., 109, pp 531-536 (1987).

(10) Aronov, V., and Benetatos, M., "Wear Resistance of Laser Treated Partially Stabilized Zirconia," ASME Preprint No. 88-Trib-58, 1988.

(11) Wei, W., Beaty, K., Vinyard, S., and Lankford, J., "Friction and Wear Testing of Ion Beam Modified Ceramics for High Temperature Low Heat Rejection Diesel Engines," Selection and Use of Wear Tests for Ceramics, ASTM, Philadelphia (1988), STP 1010, Eds. Yust, C. S., and Bayer, R. G., pp 74-87.

(12) Erdemir, A., Fenske, G. R., Erck, R. A., and Cheng, C. C., "Ion-Assisted Deposition of Silver Films on Ceramics for Friction and Wear Control," Lubr. Eng., 46, pp 23-30 (1990).

(13) Erdemir, A., Fenske, G. R., Nichols, F. A., and Erck, R. A., "Solid Lubrication of Ceramic Surfaces by IAD-Silver Coatings for Heat Engine Applications," ASME/STLE 1989 Tribology

Conference Preprint No. 89-TC-2E-1.

(14) Erdemir, A., Busch, D. E., Fenske, G. R., and Erck, R. A., "Tribological Characterization of IAD-Treated Surfaces: IAD-Silver Coatings on Ceramics, "Tribology Project Quarterly Progress Report, DOE-ECUT Tribology Program, #TRIB-ECUT 89-3, pp 96-99 (1989).

(15) Morton Thiokol, Inc., Alfa Oxide Ceramics Division, 152 Andover Street, Danvers, MA, 01923.

(16) Gates, R. S., Yellets, J. P., Deckman, D. E., and Hsu, S. M., "Considerations in Ceramic Friction and Wear Measurements," Selection and Use of Wear Tests for Ceramics, ASTM, Philadelphia (1988), STP 1010, Eds. Yust, C. S., and Bayer. R. G., pp 1-23.

(17) Fenske, G. R., Erdemir, A., Cheng, C. C., Erck, R. A., Busch, D. E., Lee, R. H., and Nichols, F. A., "Ion-Assisted Deposition of High-Temperature Lubricious Surfaces," ASME/STLE 1989 Tribology Conference Preprint No. 89-TC-2E-2.

(18) Fischer, T. E., and Tomizawa, H., "Interaction of Tribochemistry and Microfracture in the Friction and Wear of Silicon Nitride," Wear, 105, pp 29-45 (1985).

(19) Ishigaki, J., Nagata, R., and Iwasa, M., "Friction and Wear of Partially Stabilized Zirconia, "Tribology-Friction, Lubrication and Wear, Fifty Years On., Proc. Inst. Mech. Eng., London, (1987), pp. 609-614.

(20) Hannink, R. H. J., Murray, M. J., and Scott, H. G., "Friction and Wear of Partially Stabilized Zirconia: Basic Science and Practical Applications," Wear, 100, pp 355-366 (1984).

(21) Yust, C. S. and Cariggnan, F. J., "Observations on the Sliding Wear of Ceramics," ASLE Trans., 28, pp 245-252 (1984).

(22) Hamilton, G. M., and Goodman, L. E., "The Stress Field Created by a Circular Sliding Contact," J. Appl. Mech., Ser. E, 33, pp 371-376 (1966).

(23) Lim, S. M., and Ashby, M. F., "Wear Mechanism Maps," Acta Metall., 35, pp 1-24 (1987).

(24) Winer, W. O., and Ting, B. Y., Development of a Theory of Wear of Ceramics, Final Report to Oak Ridge National Laboratory, ORNL/84-7802/1, Oak Ridge, TN 1988.

(25) Brikby, I., Harrison, P., and Stevens, H., "The Effect of Surface Transformations on the Wear Behavior of Zirconia (TZP) Ceramics," Ceram. Eng. Sci. Proc., 9, pp 1431-1442 (1988).

(26) Butler, E. P., "Transformation Toughened Zirconia Ceramics," Mat. Sci. Technol., 1, pp 417-432 (1985).

(27) Cuomo, J. J., Rossnagel, S. M., and Kaufman, H. R., Handbook of Ion Beam Processing Technology, Noyes Publications, Park Ridge, NJ, USA, (1989).

(28) Griffioen, J. A., Bair, S., and Winer, W. O., "Infrared Surface Temperature Measurements in a Sliding Ceramic-Ceramic Contact," 12th Leeds-Lyon Symp. on Tribology, Butterworths, London (1986), Eds. Dowson, D., Taylor, C. M., Godet, M., and Berthe, D., pp 238-245.

A. Erdemir

"Ion-Beam-Assisted Deposition of Silver Films on Zirconia Ceramics for Improved Tribological Behavior".

FIGURE CAPTIONS

Fig. 1. Friction coefficients of pairs with and without silver film during long-range sliding tests at a velocity of 1 $m.s^{-1}$.

Fig. 2. Variation of wear rates of uncoated disks and of balls sliding against silver-coated and uncoated disks at different velocities.

Fig. 3. 3-D surface maps of wear tracks formed on (a) uncoated and (b) silver-coated zirconia disks after sliding for 71 km.

Fig. 4. (a) SEM micrograph and (b) Ag-X-ray map of track formed on silver-coated zirconia disks after sliding for 71 km.

Fig. 5. SEM micrographs of typical wear scars formed on balls while sliding against uncoated disks at (a) 0.1, (b) 0.5, (c) 1, and (d) 2 $m.s^{-1}$.

Fig. 6. High-magnification SEM micrographs of wear scars formed on zirconia balls during sliding against uncoated zirconia disks at (a) 0.1, (b) 0.5, (c) 1, and (d) 2 $m.s^{-1}$ (double arrows indicate sliding direction).

Fig. 7. SEM micrographs of (a) flake-like wear fragments found on surface of ball rubbed at 2 $m.s^{-1}$ and (b) trailing edge of same ball, showing large colonies of flake-like wear fragments accumulated around circular edge.

Fig. 8. High-magnification SEM micrographs of worn surfaces of uncoated disks after sliding at (a) 0.1, (b) 1, and (c) 2 $m.s^{-1}$ (arrows show sliding direction).

Fig. 9. SEM micrograph of wear-debris particles formed at 2 $m.s^{-1}$.

Fig. 10. (a) General and (b) close-up SEM micrographs of wear track formed on IBAD-silver-coated zirconia disk after wear testing at 1 $m.s^{-1}$ (arrow shows sliding direction).

Fig. 11. SEM micrograph of wear scar formed on zirconia ball while sliding against the silver-coated zirconia disk shown in Fig. 10.

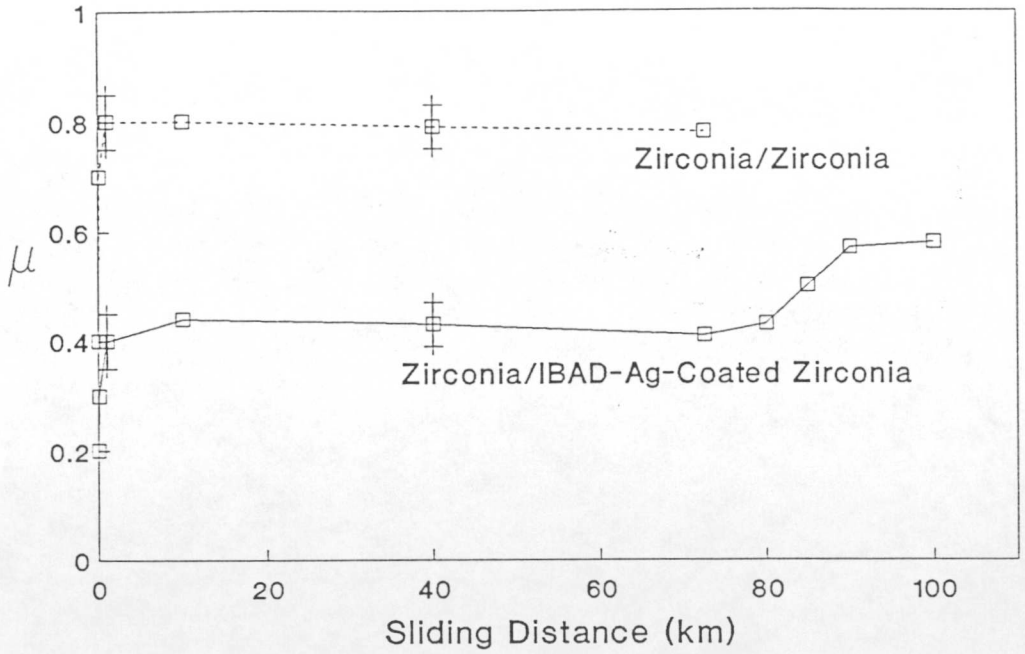
1
0.8
0.6
0.4
0.2
0
μ
Zirconia/Zirconia
Zirconia/IBAD-Ag-Coated Zirconia
0
20
40
60
80
100
Sliding Distance (km)

Fig. 1.

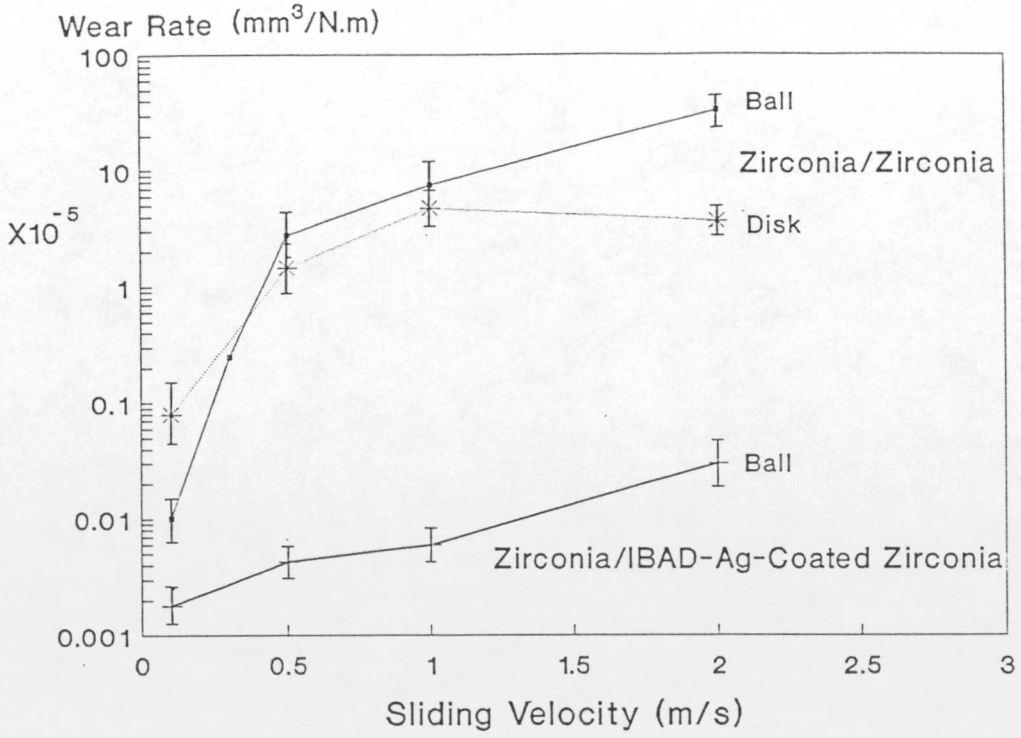
Wear Rate (mm³/N.m)
100
10
X10⁻⁵
1
0.1
0.01
0.001
0
0.5
1
1.5
2
2.5
3
Sliding Velocity (m/s)
Ball
Zirconia/Zirconia
Disk
Ball
Zirconia/IBAD-Ag-Coated Zirconia

Fig. 2.

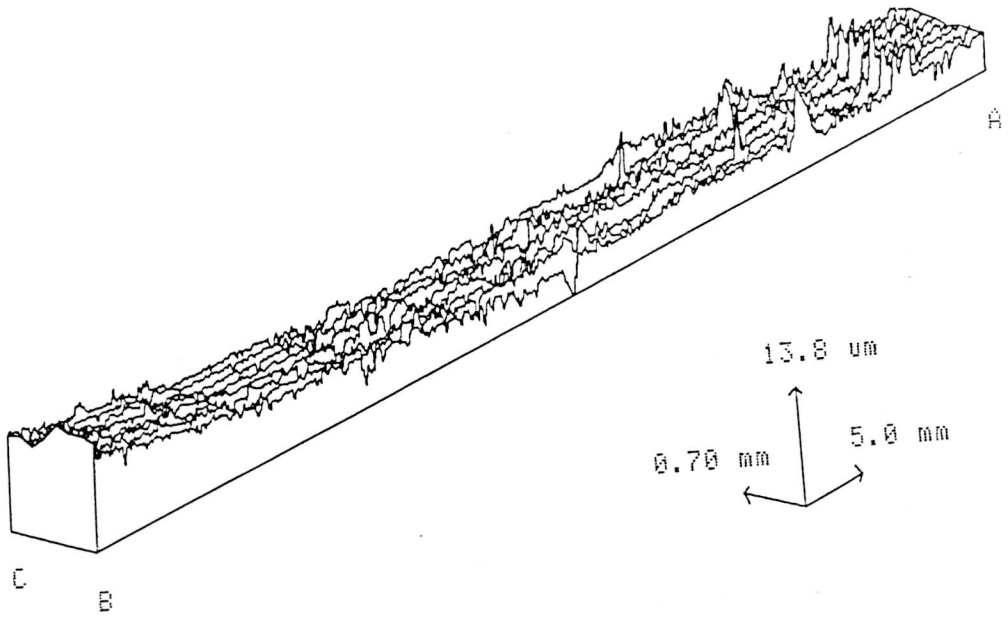

(a)

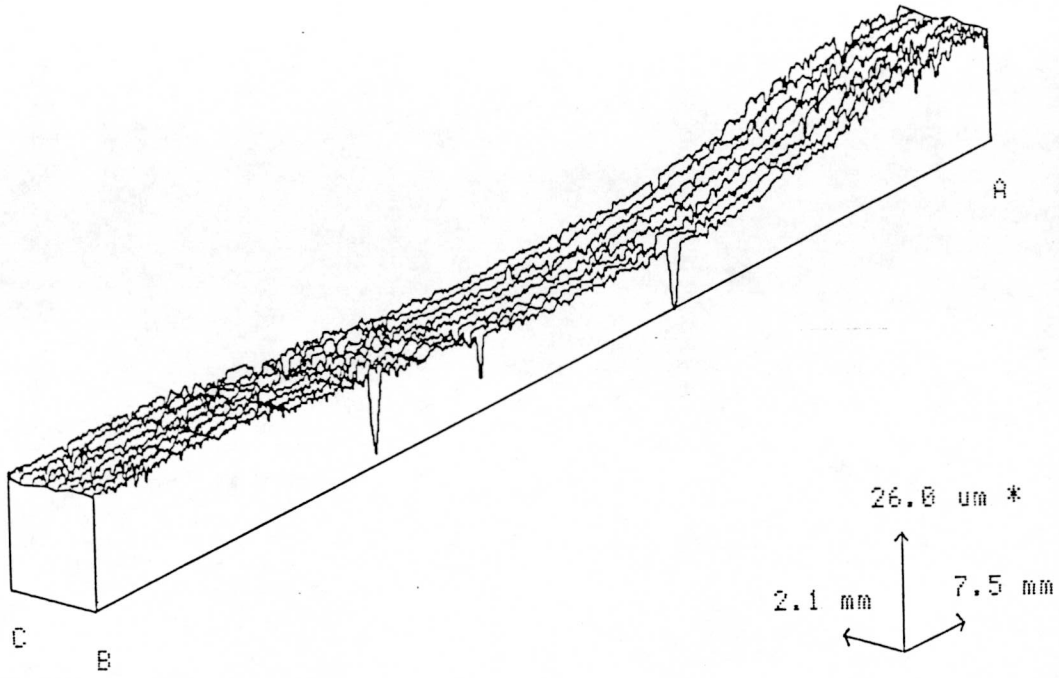

(b)

Fig. 3.

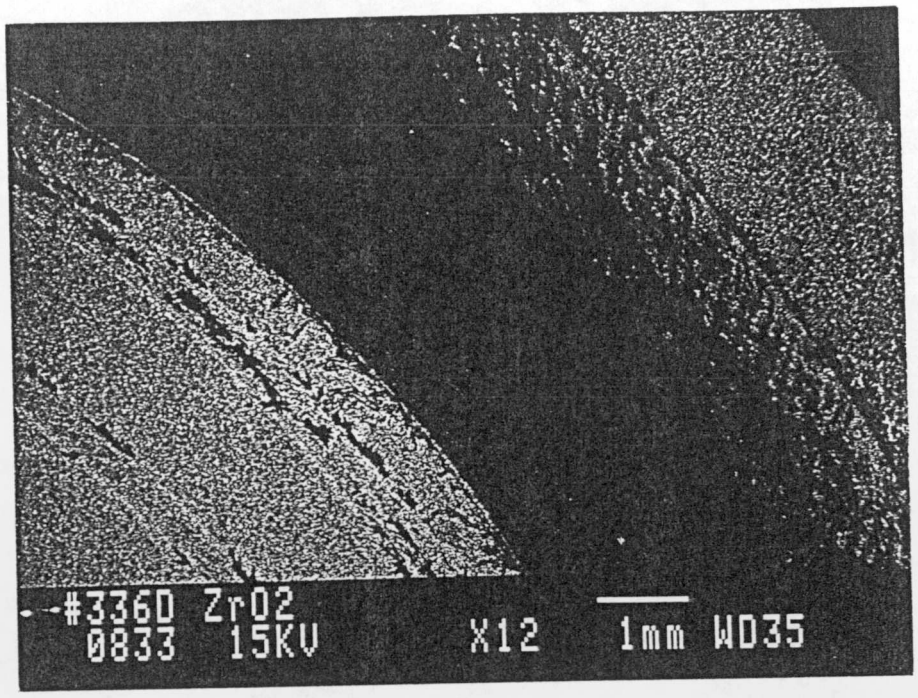
#3360 ZrO2
0833 15KV
X12
1mm WD35

(a)

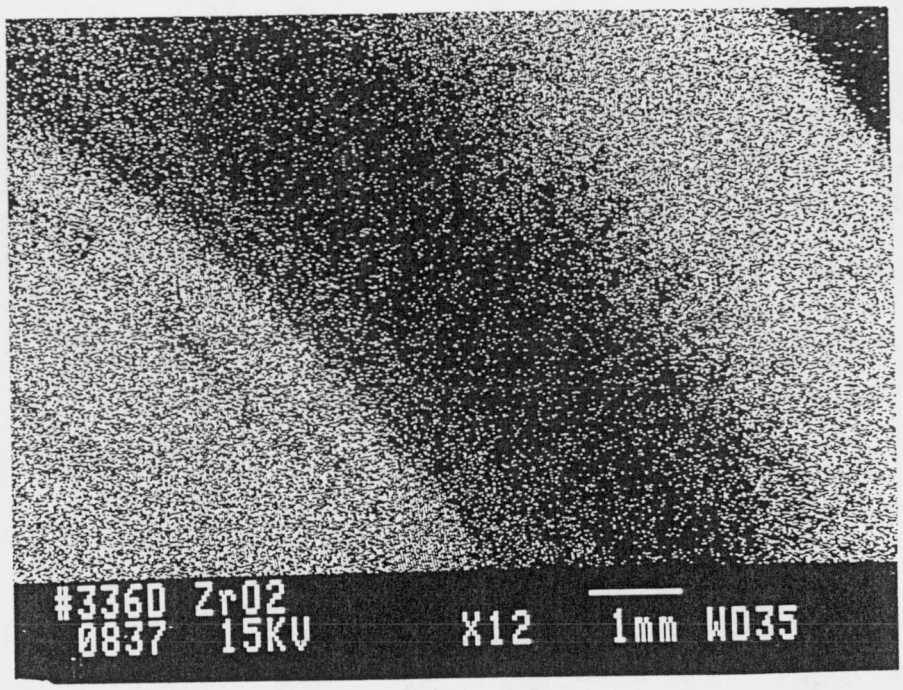
#3360 ZrO2
0837 15KV
X12
1mm WD35

(b)

Fig. 4.

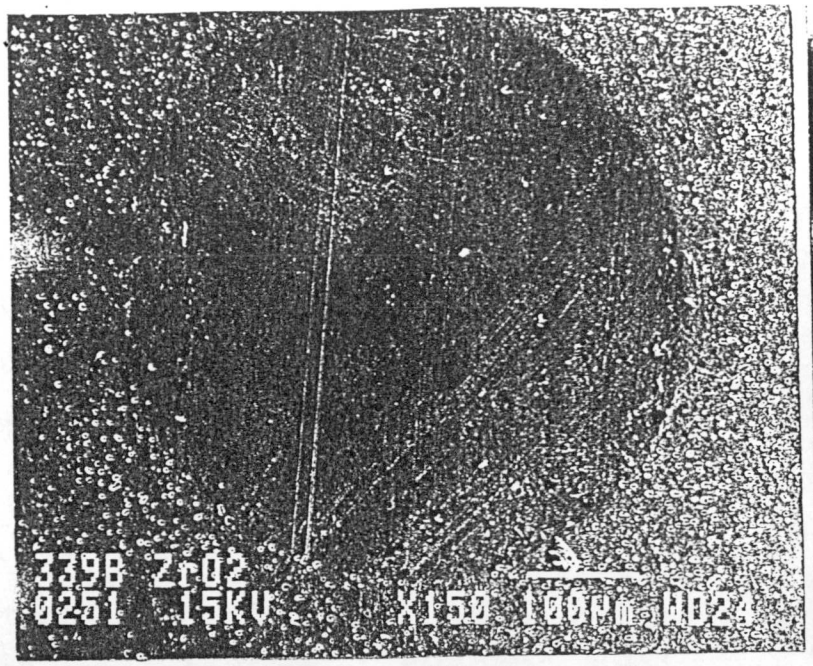
339B ZrO2
0251 15KV X150 100µm WD24

(a)

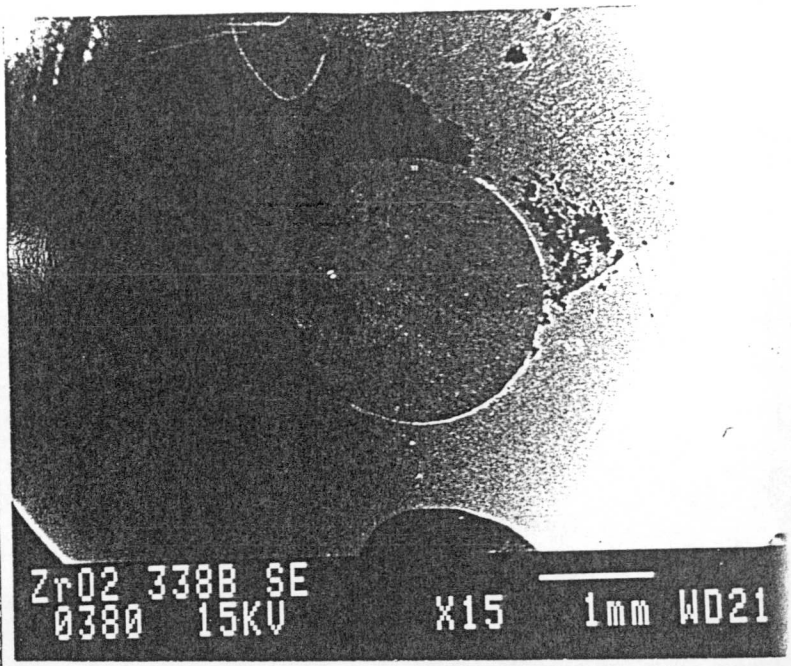
ZrO2 338B SE
0380 15KV X15 1mm WD21

(b)

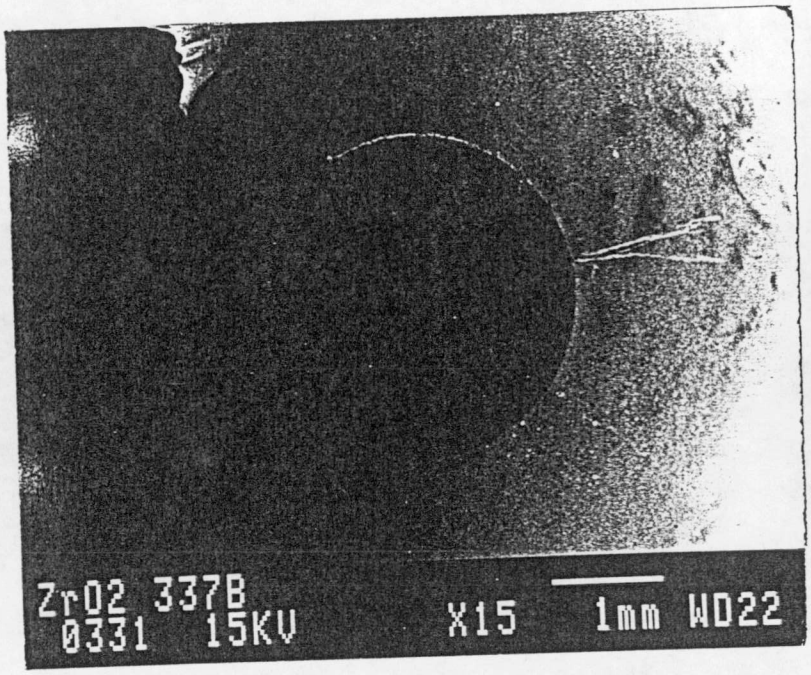
ZrO2 337B
0331 15KV X15 1mm WD22

(c)

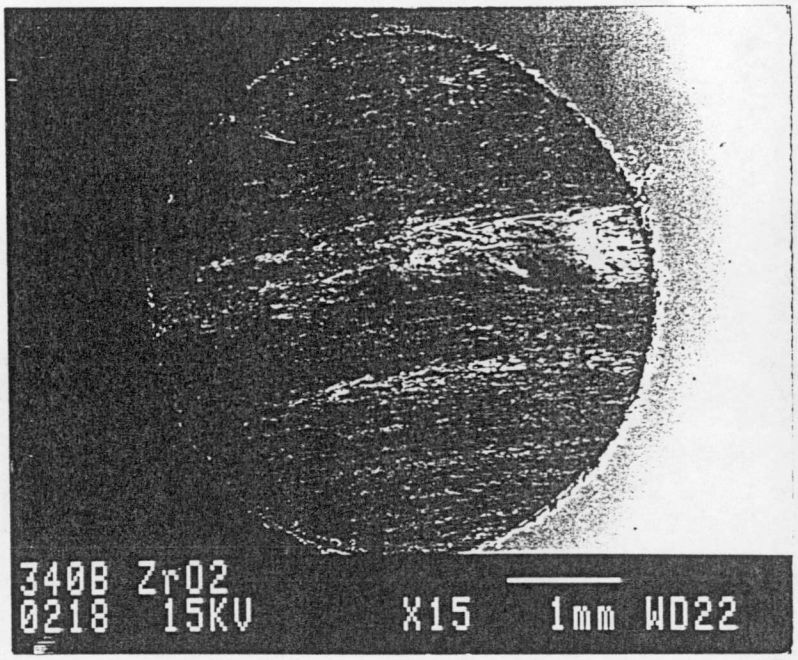
340B ZrO2
0218 15KV X15 1mm WD22

(d)

Fig. 5.

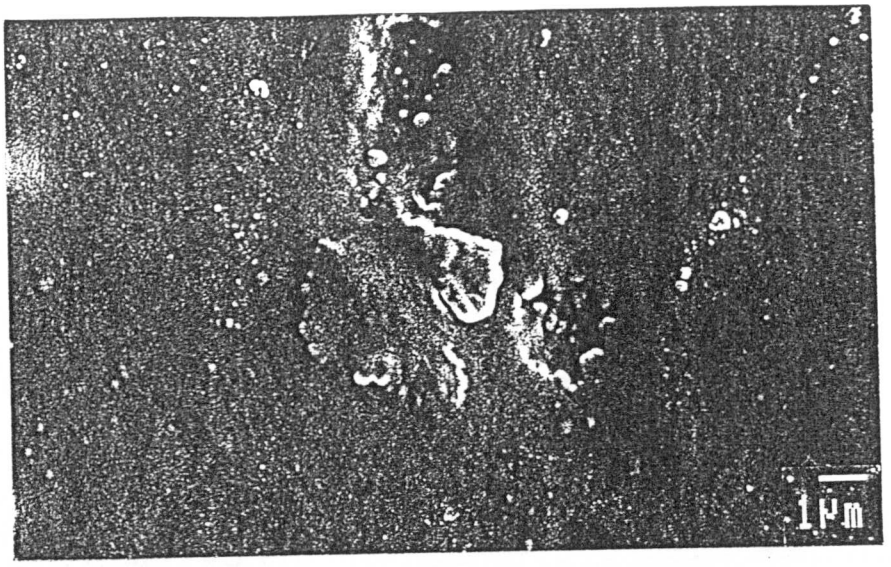

(a)

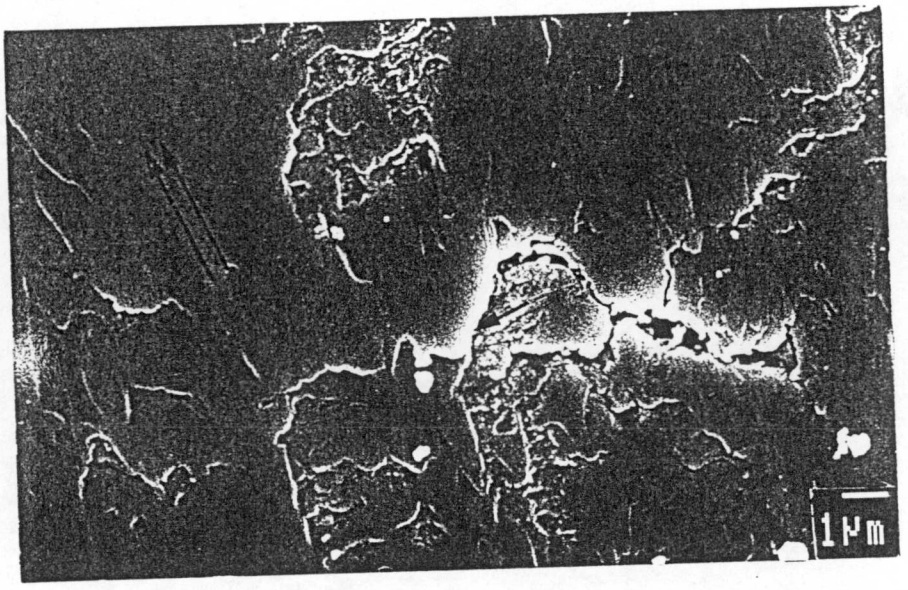

(b)

Fig. 6.

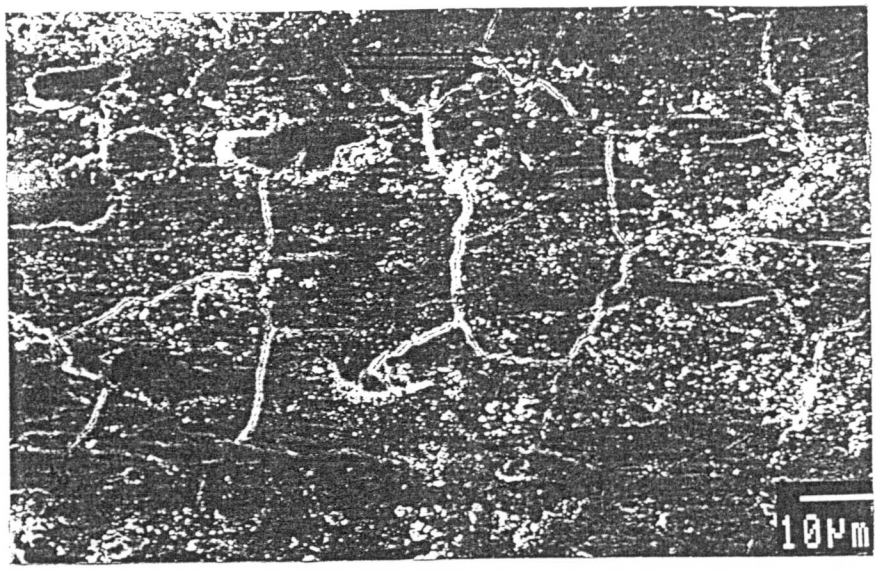

(c)

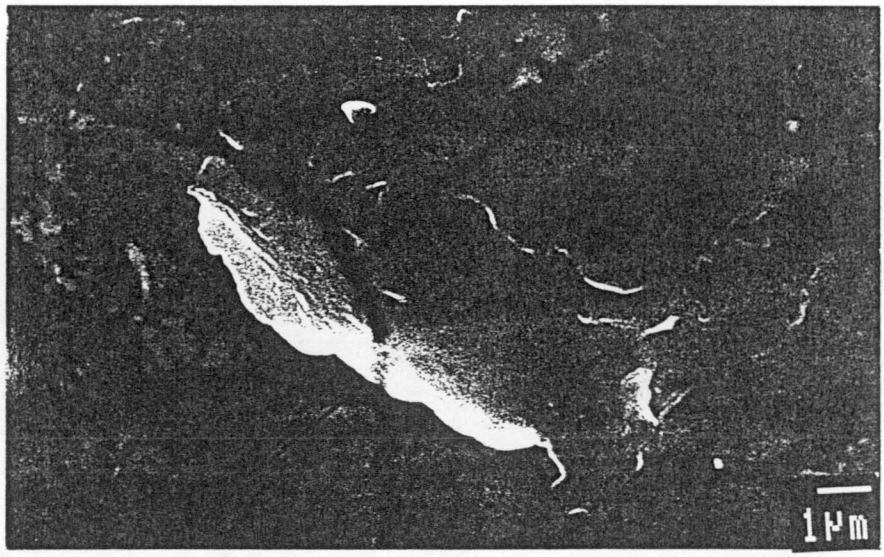

(d)

Fig. 6.

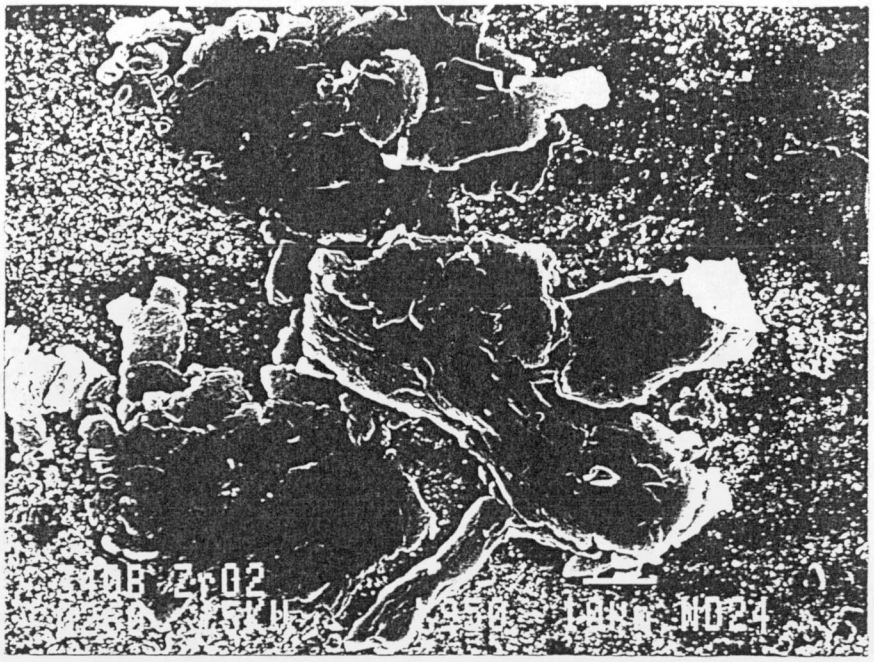

(a)

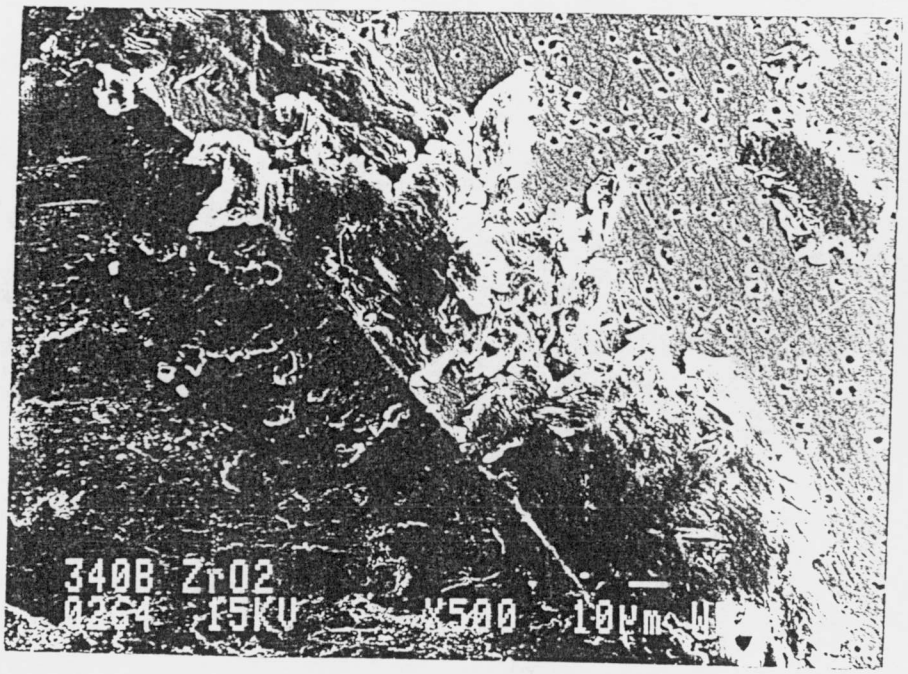

(b)

Fig. 7.

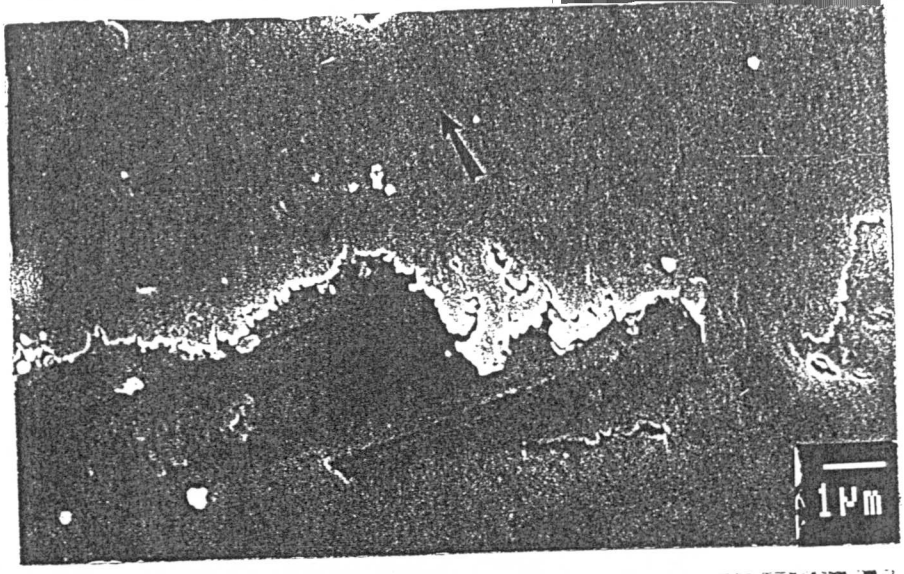

(a)

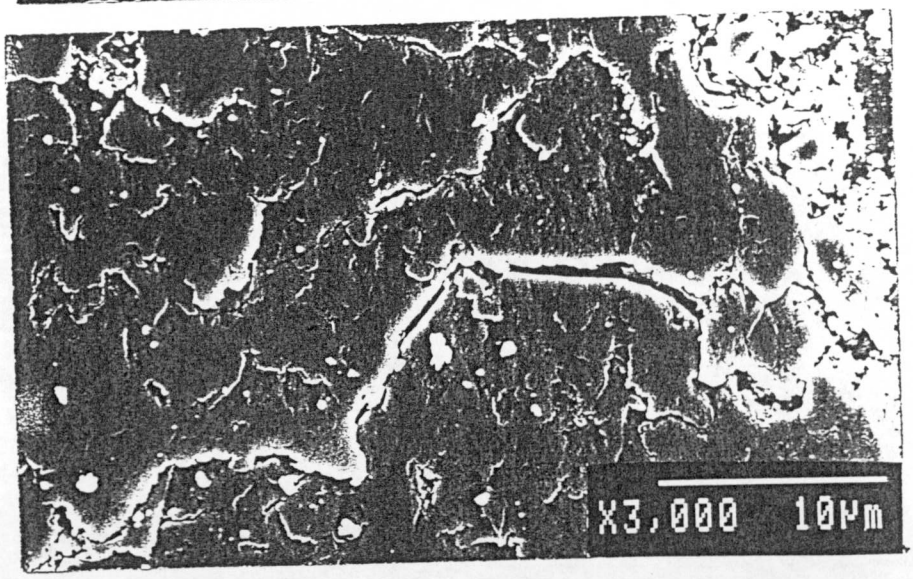

(b)

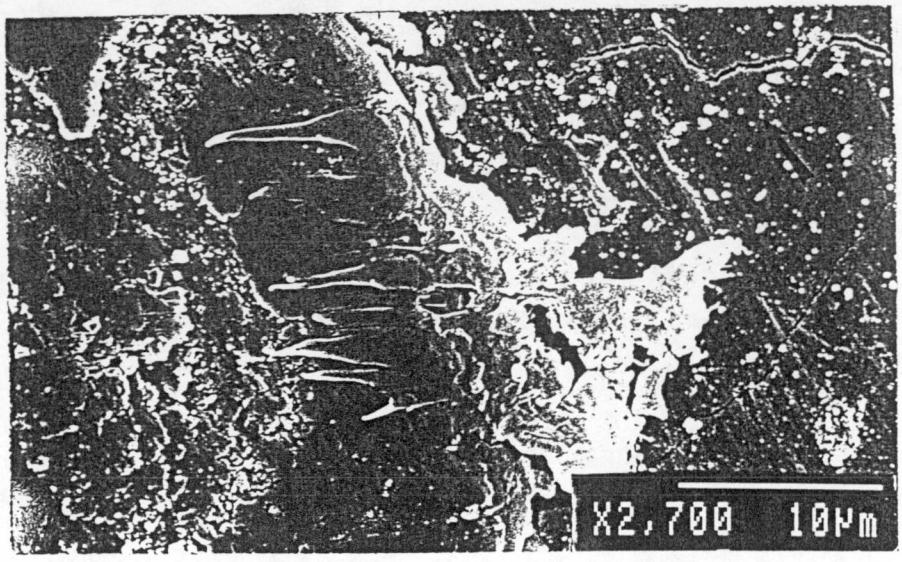

(c)

Fig. 8.

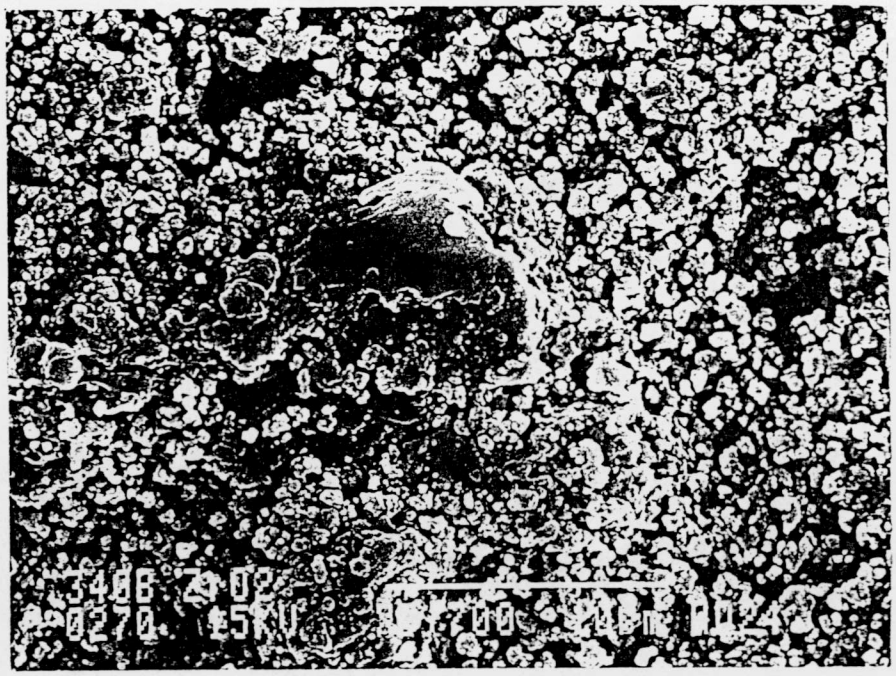

Fig. 9.

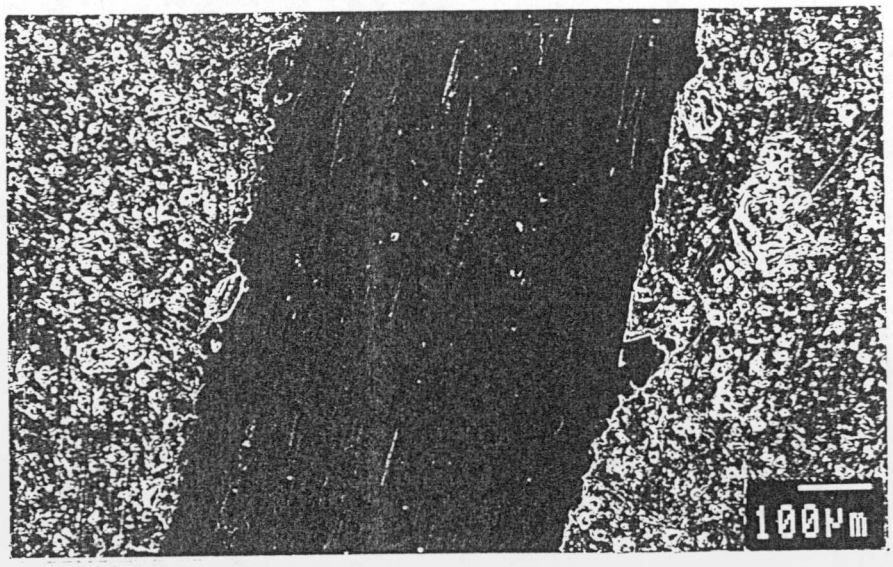

(a)

(b)

Fig. 10.

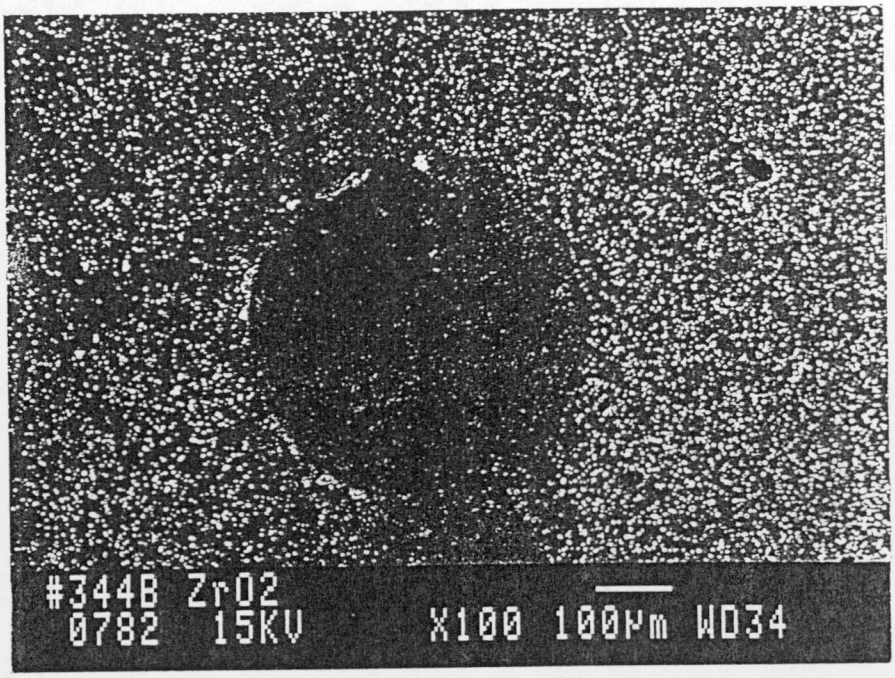

Fig. 11.